energy&fuels

Article

Cite This: Energy Fuels 2018, 32, 9551−9558

pubs.acs.org/EF

Kinetic and Thermodynamic Analyses of Sugar Cane Bagasse and Sewage Sludge Co-pyrolysis Process

Zeeshan Hameed,[†] Zaeem Aman,[†] Salman Raza Naqvi,*[,†,‡] Rumaisa Tariq,[†] Imtiaz Ali,[§] and Anas A. Makki[∥]

[†]School of Chemical and Materials Engineering, National University of Sciences and Technology, H-12, Islamabad, Pakistan

[‡]Thermal Engineering Group, Faculty of Engineering Technology, University of Twente, 7500AE Enschede, Netherlands

[§]Department of Chemical and Materials Engineering and [∥]Department of Industrial Engineering, King Abdulaziz University, Rabigh 25732, Saudi Arabia

Supporting Information

ABSTRACT: This study investigates the co-pyrolysis of sugar cane bagasse (B), sewage sludge (S), and their blends of different proportions (100% B, 70% B/30% S, 50% B/50% S, 30% B/70% S, and 100% S) through thermogravimetric analysis−differential thermal analysis at 20 °C/min. The purpose of this study to assess the synergistic effect of the addition of sugar cane bagasse into sewage sludge and investigate the co-pyrolysis process kinetics and thermodynamics by employing five major reaction mechanisms with 17 models using the Coats and Redfern method. The kinetic result indicates a synergistic effect of bagasse and sewage sludge. The active co-pyrolysis zone was divided into two reaction zones: zone I (200−400 °C) and zone II (400−600 °C). In both zones, 100% bagasse has the highest E_a (F1−F3, 20.77−106.54 kJ/mol; D1−D4, 1.59−89.27 kJ/mol; N1−N4, 2.33−43.69 kJ/mol; and P0.5−Pi, 2.15−39.88 kJ/mol) and A (F1−F3, $2.22 \times 10^{+2}$−$6.4 \times 10^{+10}$ min^{-1}; D1−D4, $3.20 \times 10^{+2}$−$3.72 \times 10^{+2}$ min^{-1}; N1−N4, $2.33 \times 10^{+2}$−$3.20 \times 10^{+2}$ min^{-1}; and P0.5−Pi, $2.33 \times 10^{+2}$−$3.20 \times 10^{+2}$ min^{-1}) compared to 100% sewage sludge E_a (F1−F3, 6.20−51.06 kJ/mol; D1−D4, 1.85−68.01 kJ/mol; N1−N4, 2.07−32.06 kJ/mol; and P0.5−Pi, 0.91−29.25 kJ/mol) and A (F1−F3, $2.66 \times 10^{+2}$−$4.0 \times 10^{+2}$ min^{-1}; D1−D4, $2.66 \times 10^{+2}$−$4.32 \times 10^{+2}$ min^{-1}; N1−N4, $2.06 \times 10^{+2}$−$2.66 \times 10^{+2}$ min^{-1}; and P0.5−Pi, $2.06 \times 10^{+2}$−$2.66 \times 10^{+2}$ min^{-1}) for all reaction mechanisms. Among blends in zones I and II, 70% B/30% S showed the highest E_a (F1−F3, 17.15−82.77 kJ/mol; D1−D4, 4.34−89.15 kJ/mol; N1−N4, 1.83−42.44 kJ/mol; and P0.5−Pi, 2.27−39.82 kJ/mol) and A (F1−F3, $2.24 \times 10^{+2}$−$3.40 \times 10^{+2}$ min^{-1}; D1−D4, $4.76 \times 10^{+2}$−$12 \times 10^{+5}$ min^{-1}; N1−N4, $2.32 \times 10^{+2}$−$2.43 \times 10^{+2}$ min^{-1}; and P0.5−Pi, $2.32 \times 10^{+2}$−$2.34 \times 10^{+2}$ min^{-1}) compared to all other blends for all reaction mechanisms.

1. INTRODUCTION

The increasing energy demand is intensifying the worth and exhaustion of fossil fuels. CO_2 originated from fossil fuels is responsible for 84% of greenhouse gas (GHG) released to the troposphere,[1] causing global warming, depletion of the ozone layer, acid rain, and other environmental pollution. Besides this, fossil fuels have limited reserves. By considering the intensified energy mandate, it is obligatory to substitute with renewable and sustainable resources, such as wastes and lignocellulosic biomass, which can assist in decreasing carbon footprints. These alternative resources have gained much attention in the recent times as a result of their wider availability, lower cost, and environmental benefits.[2]

Pakistan has a rich agriculture base. In 2016−2017, 12−14 million tons of bagasse was produced from 45 million tons of sugar cane.[3] Sugar cane bagasse has immense potential to produce biofuel and bioenergy;[4] thus, it is possible to solve energy crises for a debt-ridden economy using alternative energy sources.[5,6] Sewage sludge is another potential source of bio-oil and energy. It is composed of a large amount of organic matter;[7] besides, it also contains heavy metals, synthetic organic compounds, and pathogenic microorganisms, which are considered harmful for the ecological systems.[8] Thermochemical conversion (pyrolysis, gasification, and combustion) is the right process to remove these fatal elements and more efficiently generate biofuel.[9] Pyrolysis is superseding gasification and high-pressure liquefaction processes as a result of its potential to produce valuable bio-oil more efficiently.[10,11] However, the pyrolysis oil obtained from the biomass alone is acidic, highly reactive, viscous, and lower in heating value compared to the conventional oils. Moreover, high oxygen and water contents cause corrosion and instability; as a result of these reasons, pyrolysis oil is not used directly as fuel.[12−14]

One of the auspicious paths to gain valuable bioenergy is through co-pyrolysis. The mechanism of co-pyrolysis is similar to that of the pyrolysis process with two or more than two feedstocks. Co-pyrolysis of biomass and sewage is relatively a cost-effective process, which can reduce the landfill methane emission and other environmental pollution.[15] Co-pyrolysis of biomass is a better way to use waste materials. It can be considered as an inexpensive, harmless, and environmentally friendly process.[16] The blending ratio in a co-pyrolysis process is an important factor to realize the synergistic effects. The synergetic effect is not only influenced by the feedstock ratio but

Received: June 6, 2018
Revised: August 9, 2018
Published: August 9, 2018

DOI: 10.1021/acs.energyfuels.8b01972
Energy Fuels 2018, 32, 9551−9558

Table 1. Common Reaction Mechanisms of Solid-State Decomposition of Their Integral Form Used in the Coats and Redfern Method[20−22]

reaction mechanism and symbol	$f(\alpha)$	$g(\alpha)$
first order (n = 1), F1	$(1-\alpha)$	$-\ln(1-\alpha)$
one and a half order (n = 3/2), F1.5	$(1-\alpha)^{3/2}$	$2[(1-\alpha)^{-1/2}-1]$
second order (n = 2), F2	$(1-\alpha)^{2}$	$(1-\alpha)^{-1}-1$
third order (n = 3), F3	$(1-\alpha)^{3}$	$[(1-\alpha)^{-2}-1]/2$
parabolic law, D1	$1/2\alpha$	α^{2}
Va Lansi equation, D2	$[\ln(1-\alpha)]^{-1}$	$(1-\alpha)\ln(1-\alpha)+\alpha$
anti-Jander equation, D3 AJ	$1/2(1+\alpha)^{2/3}[(1+\alpha)^{1/3}-1]^{-1}$	$(1-2\alpha/3)-(1-\alpha)^{2/3}$
Jander equation, D3	$3/2(1-\alpha)^{2/3}[(1+\alpha)^{1/3}-1]^{-1}$	$[1-(1-\alpha)^{1/3}]^{2}$
Ginstling equation, D4	$3/2[(1-\alpha)^{-1/3}-1]^{-1}$	$1-(0.67\alpha)-(1-\alpha)^{0.67}$
Avrami−Erofeev equation (n = 1), N1	$-(1-\alpha)[-\ln(1-\alpha)]^{-1}$	$[-\ln(1-\alpha)]^{-1}$
Avrami−Erofeev equation (n = 3/2), N1.5	$3/2(1-\alpha)[-\ln(1-\alpha)]^{1/3}$	$[-\ln(1-\alpha)]^{2/3}$
Avrami−Erofeev equation (n = 2), N2	$2(1-\alpha)[-\ln(1-\alpha)]^{1/2}$	$[-\ln(1-\alpha)]^{1/2}$
Avrami−Erofeev equation (n = 3), N3	$3(1-\alpha)[-\ln(1-\alpha)]^{2/3}$	$[-\ln(1-\alpha)]^{1/3}$
contracting cylinder, PI	$2(1-\alpha)^{1/2}$	$1-(1-\alpha)^{1/2}$
contracting sphere, Pi	$3(1-\alpha)^{2/3}$	$1-(1-\alpha)^{1/3}$
power law (contracting disk), PL	1	α
Mampel power law (n = 1/2), PL0.5	$2\alpha^{1/2}$	$\alpha^{1/2}$

also affected by the pyrolytic conditions, such as the heating rate, temperature, contact time, etc.[17] However, there is no comprehensive study on the co-pyrolysis kinetics and thermodynamic behavior of sugar cane bagasse and sewage sludge blends using thermogravimetric analysis (TGA). To address scale-up issues and process challenges in the co-pyrolysis process, kinetic and thermodynamic evolution is necessary. The use of sugar cane bagasse and sewage sludge blends in a co-pyrolysis process can be seen as a potential alternative of fossil fuels as a result of its widespread availability and environmentally benign nature. Thus, the intention of this research is to explore the co-pyrolysis behavior of sugar cane bagasse and sewage sludge and to assess the synergistic effect in process kinetics and thermodynamics. Coats−Redfern is an effective method to obtain inclusive kinetic[18] and thermodynamic contours during co-pyrolysis.

2. MATERIALS AND METHODS

2.1. Raw Materials and Characterization. Sugar cane bagasse was collected from the local sugar industry located in Pakistan. Sewage sludge was collected from a membrane bioreactor (MBR) municipal wastewater treatment plant located at the National University of Science and Technology, Islamabad, Pakistan. Both samples were dried through direct sunlight for 1 week to remove excess water present in it before further treatment. After that, these samples were dried at 105 °C for a full day in an oven. Dried sugar cane bagasse and sewage sludge were ground in a ball mill for size reduction, sieved through a 1000 μm screen to obtain fine powder, and characterized through ultimate and proximate analyses. The ultimate analysis is used to find out the weight percentage of carbon, hydrogen, nitrogen, sulfur, and oxygen present in sugar cane bagasse and sewage sludge. This analysis was performed by a PerkinElmer CHNS/O 2400 elemental analyzer. Proximate analysis is used to determine the moisture, volatile matter, ash, and fixed carbon contents. In this analysis, the oven and muffle furnace are used according to the ASTM standard method. Different blends of sugar cane bagasse and sewage sludge of different weight percent ratios, such as 100% B, 70% B/30% S, 50% B/50% S, 30% B/70% S, and 100% S, were prepared. These blends were further characterized by Fourier transform infrared spectroscopy (FITR) analysis.

2.2. Co-pyrolysis Using TGA. Thermal analyses of sugar cane and sewage sludge blends were carried out in a Shimadzu DTG-60/60H thermogravimetric analyzer under nitrogen flow (200 mL/min) with a heating rate of 20 °C/min from 25 to 800 °C. For each experimental run, 10 mg of each sample was used to determine the weight loss characteristics as a function of time and temperature. The thermogravimetric analyzer consists of a sample holder placed in a programmable furnace in which the sample is placed in an alumina crucible. The sample holder is assisted by a sensitive precision balance. The sample is placed in a sample holder. The heating rate and temperature range are controlled through the programmed control panel. For accurate results and patterns, experiments were repeated thrice to evaluate their reproducibility.

2.3. Kinetic Calculations. Pyrolysis of biomass and sewage sludge blends is a complex process because of various intermediate and overlapping reactions.[19] Kinetic analysis sugar cane bagasse and sewage sludge blends are performed by the non-isothermal Coats and Redfern method. It is also known as a model fitting kinetic analysis because different reaction models are applied to determine the kinetic parameters of the pyrolysis process. It has significant importance because the exact reaction mechanism is not required in this type of model.

All kinetic analyses start with the Arrhenius law. The kinetic expression of the reaction can be expressed using eq 1

$$\frac{\mathrm{d}\alpha}{\mathrm{d}t} = k(T)f(\alpha) = A\exp\left(-\frac{E_a}{RT}\right)f(\alpha) \tag{1}$$

where t represents time, α is the degree of conversion, $\mathrm{d}\alpha/\mathrm{d}t$ shows the rate of the conversion process, E_a represents the activation energy, A is the pre-exponential factor, $f(\alpha)$ represents the conversion function, and T is the absolute temperature.

The degree of conversion (α) can be expressed in terms of weight loss as given by eq 2

$$\alpha = \frac{w_i - w_t}{w_i - w_f} \tag{2}$$

where w_i is the initial weight, w_t is the weight at any time t, and w_f is the final weight.

The Coats and Redfern method is the integral solution of eq 1, which takes the mathematical form of eq 3

$$\ln\left[\frac{g(\alpha)}{T^2}\right] = \ln\left[\frac{AR}{\beta E_a}\left(1-\frac{2RT}{E_a}\right)\right] - \frac{E_a}{RT} \tag{3}$$

where β represents the heating rate at which the pyrolysis process occurs and $g(\alpha)$ is a kinetic function.

Table 1 represents $f(\alpha)$ and $g(\alpha)$ of common reaction models used in the Coats and Redfern method.

2.4. Assessment of Synergistic Effects. Up to our knowledge, detailed kinetic analysis of biomass and sewage sludge co-pyrolysis is

DOI: 10.1021/acs.energyfuels.8b01972
Energy Fuels 2018, 32, 9551−9558

Table 2. Proximate and Ultimate Analyses of the Raw Material (Sewage Sludge and Sugar Cane Bagasse)

material	moisture (%)	volatile matter (%)	ash (%)	fixed carbon (%)	O (%)	C (%)	H (%)	N (%)	S (%)	HHV (MJ/kg)
sewage sludge	6.5	44.6	44.6	4.3	45.7	40.4	6.2	6.7	1	19.5
sugar cane bagasse	8.7	78.89	8.1	4.31	48.29	45.6	5.8	0.31	0	17.2

not discussed in the literature. Therefore, in the study herein, 17 models based on the reaction mechanism function (chemical reaction, diffusion, nucleation and growth, phase interfacial reaction, and power law) are applied to calculate the activation energy (E_a) and pre-exponential factor (A).

A synergistic effect can be estimated from the difference of the experimental and calculated conversions. In the absence of a synergistic effect, the conversion of the blend can be simply obtained from the weighted average using eq 4

$$\alpha_{mix} = x_S\alpha_S + (1 - x_S)\alpha_B \quad (4)$$

where x_S, α_S, and α_R are the fraction of sludge and conversions of sludge and sugar cane bagasse, respectively.

Similarly, the non-interacting conversion rate of the blend can be given by the relation in eq 5

$$\left.\frac{d\alpha}{dt}\right|_{mix} = x_S\left.\frac{d\alpha}{dt}\right|_S + (1 - x_S)\left.\frac{d\alpha}{dt}\right|_B \quad (5)$$

where $d\alpha/dt|_S$ and $d\alpha/dt|_B$ are the conversion rates of sludge and sugar cane bagasse, respectively.

2.5. Assessment of Thermodynamic Parameters. The thermodynamic analysis includes a change in enthalpy, change in Gibbs free energy, and change in entropy. These parameters can be calculated on the basis of kinetic data of sugar cane bagasse and sewage sludge co-pyrolysis. Equations 6 and 7 are used to determine the kinetic parameters

$$\Delta H = E_a - RT \quad (6)$$

$$\Delta G = E_a + RT_m \ln\left(\frac{K_B T_m}{hA}\right) \quad (7)$$

where K_B is the Boltzmann constant, which is equal to 1.381×10^{-23} m^2 kg s^{-2} K^{-1}, T_m is the maximum temperature at which maximum decomposition occurs, h is Planck's constant, which equals 6.626×10^{-34} m^2 kg s^{-1}, and R is the universal gas constant, which equals 8.314 J mol^{-1} K^{-1}.

$$\Delta S = \frac{\Delta H - \Delta G}{T_m} \quad (8)$$

3. RESULTS AND DISCUSSION

3.1. Proximate and Ultimate Analyses. The proximate and ultimate analyses for the sewage sludge and sugar cane bagasse are shown in Table 2. As perceived, biomass materials have diverse properties. The ash percentage of sewage sludge (44.6%) is much higher than that of sugar cane bagasse (8.1%). The moisture content is lower than 10% on a dry basis. Additionally, sugar cane bagasse has a larger amount of volatile matter (78.89%) than that of sewage sludge (44.6%). Sugar cane bagasse and sewage sludge both have a lower percentage of fixed carbon at 4.31 and 4.3%, respectively. Ash has a dubious role, to a certain extent, it can boost the efficiency by catalyzing conversion through trace elements; however, an excess amount can lower the heating value.[23,24]

Table 2 also shows that sewage sludge and sugar cane contain a large amount of oxygen (45.7 and 48.29%, respectively) and have a greater amount of carbon content (40.4 and 45.6%, respectively). Sugar cane bagasse has a lower percentage of nitrogen content (0.31%) than that of sewage sludge (6.7%). Both sewage sludge and sugar cane bagasse have a lower percentage of hydrogen content of 6.2 and 5.8%, respectively. The sulfur content of sewage sludge amounts to 1%.

The calculated high heating values of sewage sludge and sugar cane bagasse samples are 19.5 and 17.2 MJ/kg, respectively. The moisture-free sewage sludge and sugar cane bagasse samples usually contain a higher heating value range from 5 to 25 MJ/kg.[25]

3.2. FTIR. Figure 1 represented the FTIR spectra of pure sewage sludge, pure sugar cane bagasse, and their blends with

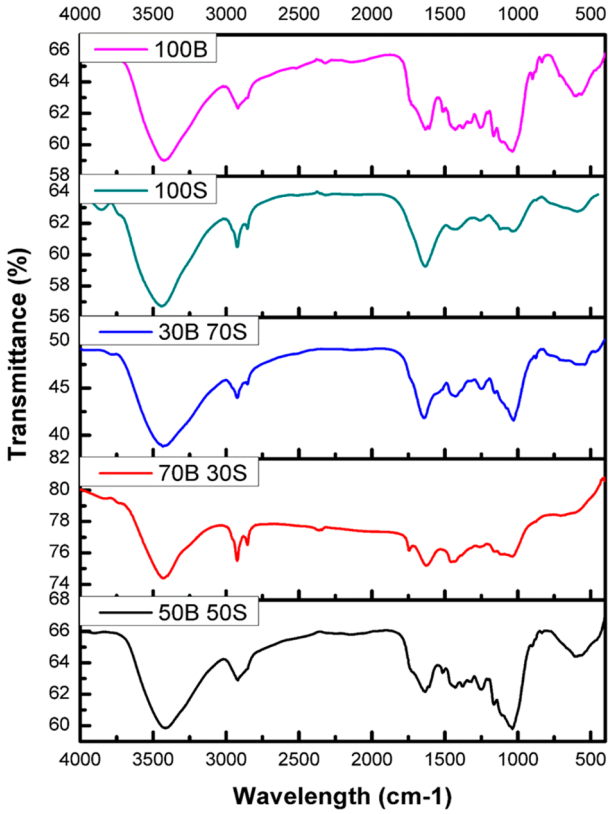

Figure 1. FTIR spectra of 100% sugar cane bagasse, 100% sewage sludge, and blends of sugar cane bagasse in the ratios of 30, 50, and 70% with sewage sludge.

different ratios. It is clearly observed that sugar cane bagasse has very vibrant peaks at 3419.33, 2880, 2310, 1634, and 1050 cm^{-1}, which give indications for the presence of −NH amide or −OH groups (3400−3500 cm^{-1}), aliphatic or aromatic groups (2500−3200 cm^{-1}), C≡N nitrile group (2200−2400 cm^{-1}), C═O aldehyde group (1650−1550 cm^{-1}), and polysaccharides (1000−1150 cm^{-1}).[26] The 100% sewage sludge also contains the −NH− amide group peak at 3419.33 cm^{-1}, aromatic or aliphatic group peak at 2950 cm^{-1}, C═O aldehyde group peak at 1634.97 cm^{-1}, and polysaccharide group at peak 1000 cm^{-1}.

The only difference is the C−N group at a peak of 3200 cm^{-1} present in 100% sewage sludge, which is not present in 100% sugar cane bagasse. The blend of 50% sewage sludge and 50% sugar cane bagasse spectrum showed peaks at 1590, 1510, and 1420 cm^{-1}, which provide evidence for benzene derivatives with

DOI: 10.1021/acs.energyfuels.8b01972
Energy Fuels 2018, 32, 9551−9558

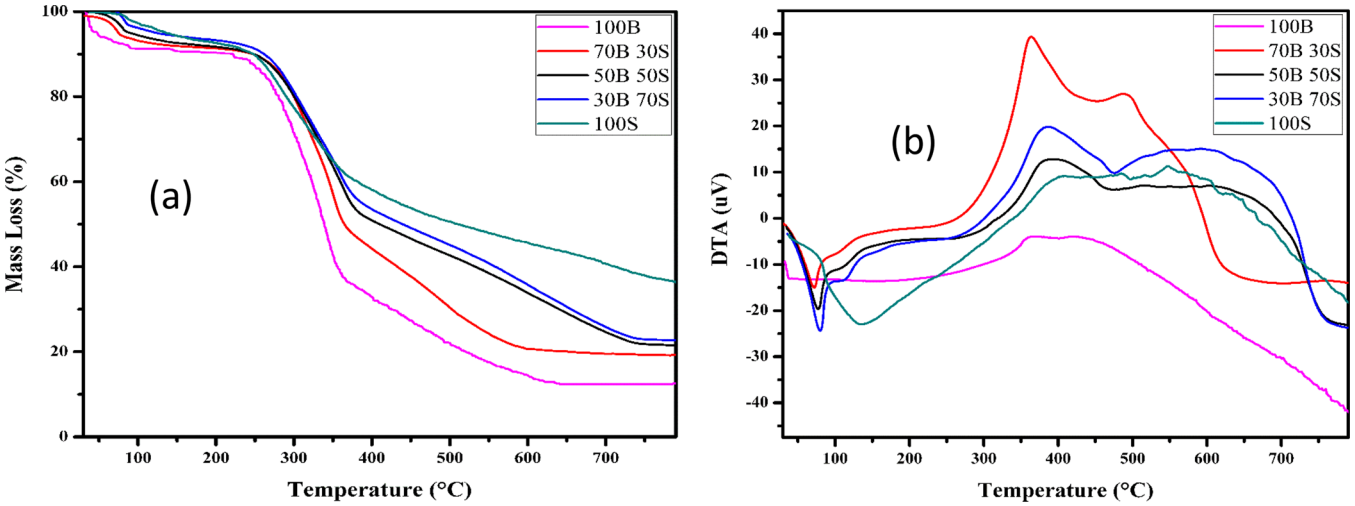

Figure 2. (a) TG and (b) DTA curves of sugar cane bagasse, sewage sludge, and their blends.

aldehyde, amide, and carboxylic acid. If the ratio of sugar cane bagasse is more than the ratio of sewage sludge, an extra peak appears at 1710 cm^{-1}, which gives identification of the C═C group with the −NH amide group at 3411.04 cm^{-1}, aromatic and aliphatic groups at 2923.24 cm^{-1}, aldehyde (C═O) group at 1627 cm^{-1}, and derivatives of benzene at 1460 cm^{-1}. If the ratio of sewage sludge is more than the ratio of sugar cane bagasse, the FTIR spectrum gives identification of the −NH amide group at 3411.04 cm^{-1}, aromatic and aliphatic groups at 2870 and 2790 cm^{-1}, C═O aldehyde group at 1642 cm^{-1}, and benzene derivatives at 1460 cm^{-1}.

In the case of biomass material, core features are credited to the existence of hemicellulose, cellulose, and lignin. The spectrum in the range of 3200−3600 cm^{-1} is due to the presence of natural fibers. The range of 1850−1250 cm^{-1} corresponds to the presence of the cellulose chain. The peaks below 1150 cm^{-1} are due to the presence of hemicellulose and cellulose.[27] The preceding part spanning 900 cm^{-1} and below is due to the asymmetrical vibrations from cycloaliphatic, aromatic, halogen, and phosphorus-containing compounds.[7]

3.3. TGA. The pyrolytic behavior of sewage sludge, sugar cane bagasse, and their mix blends during co-pyrolysis in a nitrogen environment at 20 °C/min heating rate was examined by thermogravimetric mass loss curves. Figure 2 represents the thermogravimetry (TG)−differential thermal analysis (DTA) curve of 100% sewage sludge, 100% sugar cane bagasse, and their different ratio mixtures. It can be clearly seen in Figure 2a that the curves can be separated into three parts according to the decomposition of different components. The first part starts from room temperature to 150 °C, during which moisture or light components are released. The second part can be distinguished from 200 to 600 °C, during which hemicellulose and cellulose from sugar cane bagasse while organic materials (biodegradable or non-biodegradable) from sewage sludge degrade simultaneously. This part is considered as the main decomposition part or active pyrolysis zone because a greater percentage of mass loss occurs in this zone.[28−30] This active pyrolysis zone can be subdivided into two temperature phases. Phase I starts from 200 to 400 °C, during which hemicellulose from sugar cane and biodegradable organic compounds, such as protein, polysaccharides, carboxylic acid, and silicates, from sewage sludge degrade. The second phase (400−600 °C) is where cellulose from bagasse and non-biodegradable organic material from sewage sludge thermally decompose.[31,32] It is visibly depicted from TGA curves that 100% sugar cane bagasse started to decompose prior to 100% sewage sludge and all other blends in the main decomposition zone because sugar cane bagasse being a lignocellulosic material is composed of cellulose, hemicellulose, and lignin, which are arranged in the macromolecular structure with comparatively weak bonds that break at a higher temperature.[33] The lignin from the bagasse side continued to degrade, while the inorganic material from the sewage sludge side decomposed above 600 °C.

Figure 2b shows the DTA of 100% sugar cane bagasse, 100% sewage sludge, and their blends. It gives information about the gain or loss of heat during the degradation process, indicating endothermicity or exothermicity of the reactions. It also predicts the temperature at which the maximum mass loss occurs. It also gives information about the percentage of mass loss at each stage.[34,35] The 100% bagasse and 100% sewage sludge show endothermic peaks at 120 and 97 °C with 6.5 and 6% mass losses, respectively. Different blends of bagasse and sewage sludge (70% B/30% S, 50% B/50% S, and 30% B/70% S) gave an endothermic reaction at a temperature of 95 °C with a mass loss of 6% as a result of vaporization of water and devolatilization of lighter components. As the temperature increased from 200 °C, the decomposition reactions changed from endothermic to exothermic. The 100% bagasse and 100% sewage sludge give peak temperatures at 360 and 370 °C with 55.5 and 32% mass loss in the 200−400 °C range and 420 and 510 °C with 27 and 20% mass loss in the range of 400−600 °C, respectively. The DTA curves of 70% B/30% S, 50% B/50% S, and 30% B/70% S give peak temperatures at 340, 380, and 370 °C with 50, 48, and 46% mass loss for the 200−400 °C region and 470, 510, and 530 °C with 22, 23, and 24% mass loss for the 400−600 °C region, respectively.

3.4. Kinetic Analysis. To estimate the impact of the blending ratio on the pyrolysis characteristics and kinetics, the Coats and Redfern method was implemented to obtain an inclusive approach to the kinetic profiles. It is the non-isothermal model-fitting approach, which is used to calculate the activation energy E_a and pre-exponential factor A and reaction mechanisms $f(\alpha)$.[36] E_a and A for a certain reaction mechanism can be indicated by the linear regression coefficient of determination (R^2), which was determined from the TGA data of sugar cane bagasse and sewage sludge co-pyrolysis, as displayed in Table S1

DOI: 10.1021/acs.energyfuels.8b01972
Energy Fuels 2018, 32, 9551−9558

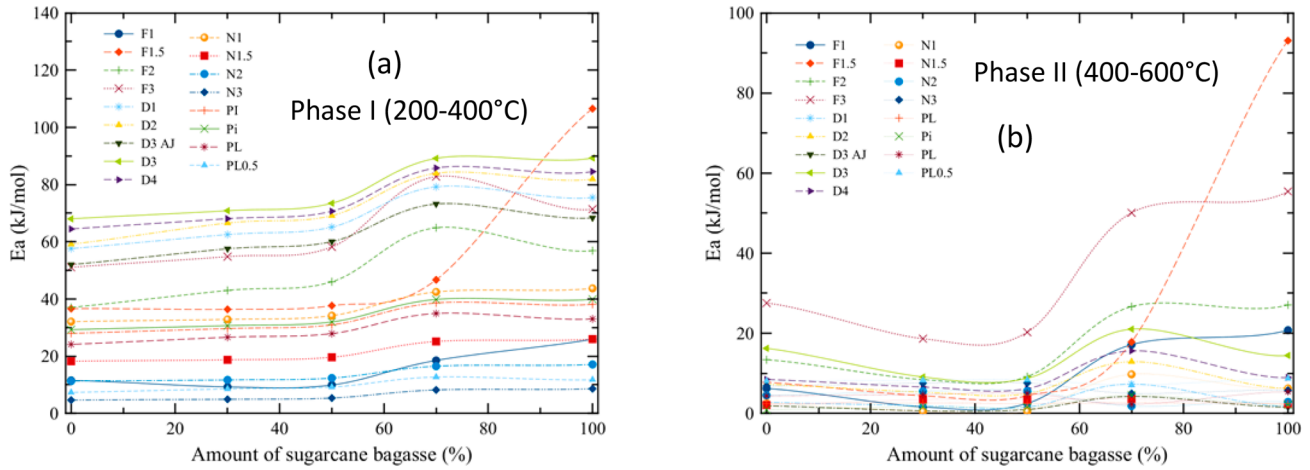

Figure 3. Variation of activation energies of different models with blending ratios in (a) phase I and (b) phase II.

of the Supporting Information. To calculate the kinetic parameters, 17 reaction mechanisms were investigated using $\ln[g(\alpha)/T^2]$ versus $1/T$ plots at 20 °C/min. E_a was obtained from the slope, whereas the intercept gives the factor A. The precision of fitting is based on R^2, and the specified range for the correct plot is 0.90−0.99.[37]

For pyrolysis of 100% bagasse, 100% sludge, and their blends, the mass loss could be regarded as a two-step process with individual E_a, A, and linear regression R^2 for each phase, 200−400 and 400−600 °C. For both phases, usually 100% bagasse has the highest E_a and A compared to 100% sewage sludge for all reaction mechanisms. For this reason, the blend of 70% bagasse/30% sewage sludge has the highest values and the blend of 30% sugar cane bagasse/70% sewage sludge has the lowest values of the activation energy and pre-exponential factors among all other blends of bagasse and sewage sludge for all reaction mechanisms. In phase I, from 200 to 400 °C, the highest E_a obtained is 89.27, 89.15, 73.46, and 70.85 kJ/mol and the pre-exponential factor is $2.42 \times 10^{+4}$, $1.27 \times 10^{+3}$, 62, and 30 min^{-1} with the Jander equation (three-dimensional diffusion mechanism) for 100, 70, 50, and 30% bagasse, respectively. In this phase, the lowest E_a and A obtained from the Avrami−Erofeev equation (nucleation and growth; $n = 3$) mechanism for 100, 70, 50, and 30% bagasse are 8.61, 8.18, 5.35, and 4.91 kJ/mol and 23, 23, 22, and 23 min^{-1}, and the regression coefficient of determination R^2 remains in the range of 0.90−0.99 for all given reaction mechanisms.

In phase II, from 400 to 600 °C, A and R^2 remain the same for all 100% bagasse, 100% sewage sludge, and their different blends. The value of the factor A for 100, 70, 50, and 30% bagasse is 32, 32, 26, and 28 min^{-1}, respectively. The value of the highest E_a for 100, 70, 50, and 30% bagasse is 55.42, 50.09, 20.27, and 18.64 kJ/mol, respectively, for the third-order reaction mechanism (cf. Figure 3).

3.5. Synergistic Effect. The yield of the volatiles as a function of the blending ratio is given in Figure 4. The amounts of volatiles generated during co-pyrolysis are different from those estimated for the corresponding non-interacting blends. This synergy originated from the interplay of sugar cane bagasse and sewage sludge components. These results endorse the variation in activation energies given in Figure 3 during phases I and II. Overall, the synergistic effect was more pronounced when 70% sludge was added to the sugar cane bagasse with higher activation energy. The 50% sludge had a slighter positive

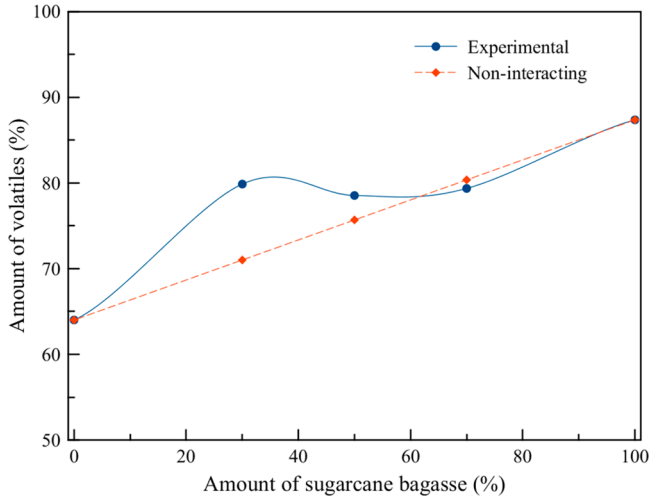

Figure 4. Yield of volatiles from different blending ratios of sewage sludge with sugar cane bagasse.

effect on the pyrolysis. The increase in the devolatilization by adding sewage sludge can be explained on the basis of the catalytic effect as a result of the metals of ash present in sewage sludge.

In Figure 5, the difference in the experimental and calculated conversions and conversion rates is shown. The departure of conversion and conversion rate differences from the theoretical values for 70% B and 30% S indicate the synergistic effect. It can be observed that the conversion of 30% B/70% S has a negative interaction, while the conversion rate interacts positively.

3.6. Thermodynamic Analysis. The thermodynamic parameters consisted of changes in enthalpy ΔH, Gibbs free energy ΔG, and entropy ΔS, which can be measured on the basis of the peak temperature obtained from the DTA (Figure 6). This temperature is categorized as the temperature at which the highest rate of mass loss was achieved.[38] The thermodynamic parameters of the thermal disintegration of bagasse, sewage sludge, and their blends of different ratios for all 17 reaction mechanisms for two distinct phases are listed in Table S2 of the Supporting Information. In phase I, from 200 to 400 °C, the values of ΔH are usually greater than the change of enthalpies obtained from phase II, from 400 to 600 °C, for all reaction mechanisms used in the Coats and Redfern method. In second phase, ΔH is usually lower or negative. ΔS is negative in both

DOI: 10.1021/acs.energyfuels.8b01972
Energy Fuels 2018, 32, 9551−9558

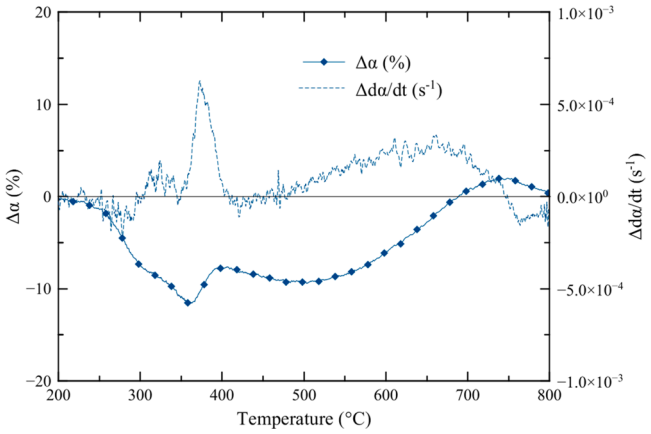

Figure 5. Conversion and conversion rate deviation of 30% B and 70% S.

phases. The highest values of ΔH and ΔG for 100, 70, 50, and 30% bagasse from the Jander equation (three-dimensional reaction mechanism) are 86.36, 86.25, 70.67, and 67.94 kJ/mol and 146.08, 154.14, 137.91, and 140.36 kJ/mol, respectively, in phase I. The highest values of ΔH and ΔG for 100, 70, 50, and 30% bagasse from the third-order reaction mechanism are 23.09, 22.63, 5.90, and 4.94 kJ/mol and 123.51, 124.10, 88.54, and 92. 81 kJ/mol, respectively, in phase II. ΔH represented the endothermicity and exothermicity of reaction mechanisms, while ΔG provided information about the increase in the total energy of the system as the reactants were consumed and the activated complex was formed. Low activation ΔS showed that the solid material faced various chemical and physical changes in the state of its thermodynamic equilibrium. In this condition, the waste and biomass showed less reactivity, with more time required to form the activated complex.[39] ΔS can also tell the degree of arrangement of the carbon deposits present in sewage sludge and biomass. Specifically, the negative values of ΔS of the formation indicate that the activated complex can be categorized by a much developed "degree of arrangement". All negative values of ΔS demonstrated that the activated complex of sewage sludge, bagasse, and their blends had a more ordered structure compared to the preliminary constituent and the pyrolysis process involved a chaotic structure to a well-ordered structure.[40]

4. CONCLUSION

This study investigates the co-pyrolysis of sugar cane bagasse (B), sewage sludge (S), and their blends of different proportions (100% B, 70% B/30% S, 50% B/50% S, 30% B/70% S, and 100% S) through TGA−DTA at 20 °C/min. Five major reaction mechanisms with 17 models were employed using the Coats and

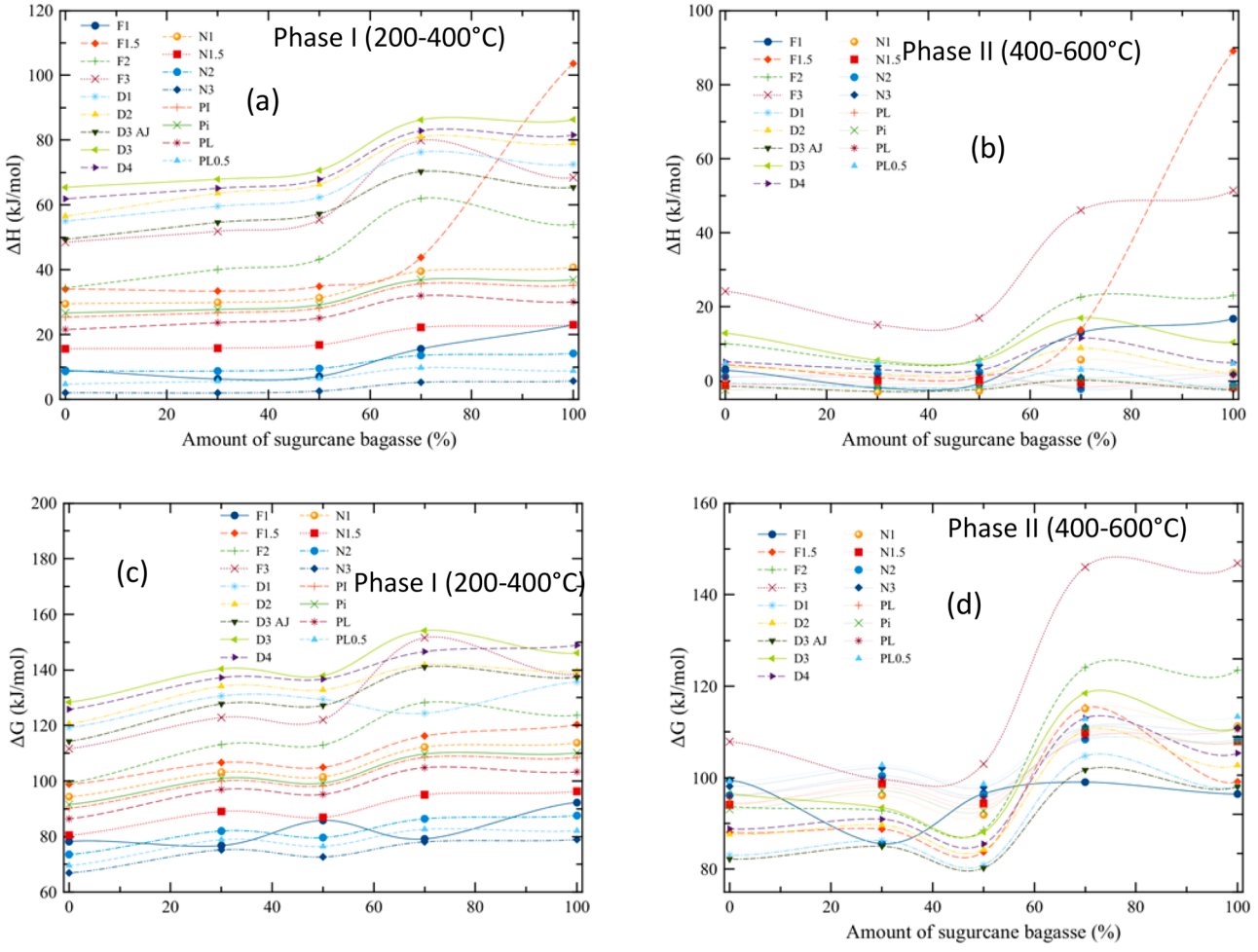

Figure 6. Changes in enthalpy (ΔH) and Gibb's free energy (ΔG) of different blending ratios of sewage sludge with sugar cane bagasse in (a and c) phase I and (b and d) phase II.

DOI: 10.1021/acs.energyfuels.8b01972
Energy Fuels 2018, 32, 9551−9558

Redfern method. The active co-pyrolysis zone was divided into two reaction zones: zone I (200−400 °C) and zone II (400−600 °C). Sugar cane bagasse behaves substantially different from sewage sludge during co-pyrolysis in terms of mass loss, maximum reactivity temperature, and amount of volatiles. The results indicate the following: (1) The thermochemical reactivity of sugar cane bagasse behaves substantially different from sewage sludge in the co-pyrolysis performance, such as mass loss, maximum reactivity temperature, and amount of volatiles. (2) The addition of bagasse in sewage sludge has an influence on the thermal behavior of the co-pyrolysis process. The synergistic effect was more pronounced when 70% sludge was added to the sugar cane bagasse. (3) The difference in the experimental and calculated conversions and conversion rates is used to quantify the synergistic effect during co-pyrolysis of sewage sludge and sugar cane bagasse. The promoting effect of volatile formation can be seen for 30% B/70% S blends. (4) ΔH and ΔG values are usually greater in zone II (400−600 °C) than zone I (200−400 °C) for all reaction mechanisms used in the Coats and Redfern method. In the second phase, the enthalpy ΔH is usually lower or a negative value. The negative values of ΔS demonstrated the formation of the activated complex of sugar cane bagasse, sewage sludge, and their blends.

■ ASSOCIATED CONTENT

Supporting Information

The Supporting Information is available free of charge on the ACS Publications website at DOI: 10.1021/acs.energyfuels.8b01972.

Kinetic parameters of 100% bagasse, 100% sewage sludge, and their blends with different proportions (Table S1) and thermodynamic parameters of 100% sewage sludge, 100% bagasse, and their blends of different ratios (Table S2) (PDF)

■ AUTHOR INFORMATION

Corresponding Author

*E-mail: s.r.naqvi@utwente.nl and/or salman.raza@scme.nust.edu.pk.

ORCID

Salman Raza Naqvi: 0000-0003-4035-181X

Notes

The authors declare no competing financial interest.

■ ACKNOWLEDGMENTS

The authors acknowledge the National University of Sciences and Technology, Pakistan.

■ REFERENCES

(1) Coal Industry Advisory Board. *21st Century Coal, Advanced Technology and Global Energy Solution, Insights Series 2013*; OECD/IEA: Paris, France, 2013.

(2) Jayaraman, K.; Gokalp, I.; Petrus, S.; Belandria, V.; Bostyn, S. Energy Recovery Analysis from Sugar Cane Bagasse Pyrolysis and Gasification Using Thermogravimetry, Mass Spectrometry and Kinetic Models. *J. Anal. Appl. Pyrolysis* **2018**, *132*, 225−236.

(3) Haseeb, M. Bagasse—An Answer to Pakistan's Declining Economy and Energy Crisis. *Technol. Times Pak.* **2018**.

(4) Brandão, F. L.; Verissimo, G. L.; Leite, M. A. H.; Leiroz, A. J. K.; Cruz, M. E. Computational Study of Sugarcane Bagasse Pyrolysis Modeling in a Bubbling Fluidized Bed Reactor. *Energy Fuels* **2018**, *32* (2), 1711−1723.

(5) Naqvi, M.; Yan, J.; Dahlquist, E.; Naqvi, S. R. Waste Biomass Gasification Based Off-Grid Electricity Generation: A Case Study in Pakistan. *Energy Procedia* **2016**, *103*, 406−412.

(6) Naqvi, S. R.; Jamshaid, S.; Naqvi, M.; Farooq, W.; Niazi, M. B. K.; Aman, Z.; Zubair, M.; Ali, M.; Shahbaz, M.; Inayat, A.; Afzal, W. Potential of Biomass for Bioenergy in Pakistan Based on Present Case and Future Perspectives. *Renewable Sustainable Energy Rev.* **2018**, *81* (Part 1), 1247−1258.

(7) Fonts, I.; Azuara, M.; Gea, G.; Murillo, M. B. Study of the Pyrolysis Liquids Obtained from Different Sewage Sludge. *J. Anal. Appl. Pyrolysis* **2009**, *85* (1−2), 184−191.

(8) Huang, H.; Yuan, X. The Migration and Transformation Behaviors of Heavy Metals during the Hydrothermal Treatment of Sewage Sludge. *Bioresour. Technol.* **2016**, *200*, 991−998.

(9) Manzano-Agugliaro, F.; Alcayde, A.; Montoya, F. G.; Zapata-Sierra, A.; Gil, C. Scientific Production of Renewable Energies Worldwide: An Overview. *Renewable Sustainable Energy Rev.* **2013**, *18*, 134−143.

(10) Ali, I.; Bahadar, A. Red Sea Seaweed (Sargassum Spp.) Pyrolysis and Its Devolatilization Kinetics. *Algal Res.* **2017**, *21*, 89−97.

(11) Kan, T.; Strezov, V.; Evans, T. J. Lignocellulosic Biomass Pyrolysis: A Review of Product Properties and Effects of Pyrolysis Parameters. *Renewable Sustainable Energy Rev.* **2016**, *57*, 1126−1140.

(12) Fan, L.; Chen, P.; Zhang, Y.; Liu, S.; Liu, Y.; Wang, Y.; Dai, L.; Ruan, R. Fast Microwave-Assisted Catalytic Co-Pyrolysis of Lignin and Low-Density Polyethylene with HZSM-5 and MgO for Improved Bio-Oil Yield and Quality. *Bioresour. Technol.* **2017**, *225*, 199−205.

(13) Naqvi, S. R.; Uemura, Y.; Osman, N. B.; Yusup, S.; Nuruddin, M. F. Physiochemical Properties of Pyrolysis Oil Derived from Fast Pyrolysis of Wet and Dried Rice Husk in a Free Fall Reactor. *Appl. Mech. Mater.* **2014**, *625*, 604−607.

(14) Önal, E.; Uzun, B. B.; Pütün, A. E. Bio-Oil Production via Co-Pyrolysis of Almond Shell as Biomass and High Density Polyethylene. *Energy Convers. Manage.* **2014**, *78*, 704−710.

(15) Zhang, W.; Yuan, C.; Xu, J.; Yang, X. Beneficial Synergetic Effect on Gas Production during Co-Pyrolysis of Sewage Sludge and Biomass in a Vacuum Reactor. *Bioresour. Technol.* **2015**, *183*, 255−258.

(16) Demirbas, A.; Arin, G. An Overview of Biomass Pyrolysis. *Energy Sources* **2002**, *24* (5), 471−482.

(17) Abnisa, F.; Wan Daud, W. M. A. A Review on Co-Pyrolysis of Biomass: An Optional Technique to Obtain a High-Grade Pyrolysis Oil. *Energy Convers. Manage.* **2014**, *87*, 71−85.

(18) Naqvi, S. R.; Uemura, Y.; Osman, N.; Yusup, S. Kinetic Study of the Catalytic Pyrolysis of Paddy Husk by Use of Thermogravimetric Data and the Coats−Redfern Model. *Res. Chem. Intermed.* **2015**, *41* (12), 9743−9755.

(19) Ranzi, E.; Cuoci, A.; Faravelli, T.; Frassoldati, A.; Migliavacca, G.; Pierucci, S.; Sommariva, S. Chemical Kinetics of Biomass Pyrolysis. *Energy Fuels* **2008**, *22* (6), 4292−4300.

(20) Ebrahimi-Kahrizsangi, R.; Abbasi, M. H. Evaluation of Reliability of Coats−Redfern Method for Kinetic Analysis of Non-isothermal TGA. *Trans. Nonferrous Met. Soc. China* **2008**, *18* (1), 217−221.

(21) Khawam, A.; Flanagan, D. R. Complementary Use of Model-Free and Modelistic Methods in the Analysis of Solid-State Kinetics. *J. Phys. Chem. B* **2005**, *109* (20), 10073−10080.

(22) Vlaev, L.; Nedelchev, N.; Gyurova, K.; Zagorcheva, M. A Comparative Study of Non-Isothermal Kinetics of Decomposition of Calcium Oxalate Monohydrate. *J. Anal. Appl. Pyrolysis* **2008**, *81* (2), 253−262.

(23) Vassilev, S. V.; Baxter, D.; Andersen, L. K.; Vassileva, C. G. An Overview of the Chemical Composition of Biomass. *Fuel* **2010**, *89* (5), 913−933.

(24) Fonts, I.; Azuara, M.; Gea, G.; Murillo, M. B. Study of the Pyrolysis Liquids Obtained from Different Sewage Sludge. *J. Anal. Appl. Pyrolysis* **2009**, *85* (1−2), 184−191.

(25) Demirbaş, A. Calculation of Higher Heating Values of Biomass Fuels. *Fuel* **1997**, *76* (5), 431−434.

DOI: 10.1021/acs.energyfuels.8b01972
Energy Fuels 2018, 32, 9551−9558

(26) Alvarez, J.; Amutio, M.; Lopez, G.; Bilbao, J.; Olazar, M. Fast Co-Pyrolysis of Sewage Sludge and Lignocellulosic Biomass in a Conical Spouted Bed Reactor. *Fuel* **2015**, *159*, 810−818.
(27) Mothé, C. G.; Miranda, I. C. Characterization of Sugarcane and Coconut Fibers by Thermal Analysis and FTIR. *J. Therm. Anal. Calorim.* **2009**, *97* (2), 661−665.
(28) Ali, I.; Bahaitham, H.; Naebulharam, R. A Comprehensive Kinetics Study of Coconut Shell Waste Pyrolysis. *Bioresour. Technol.* **2017**, *235*, 1−11.
(29) de Oliveira Silva, J.; Filho, G. R.; da Silva Meireles, C.; Ribeiro, S. D.; Vieira, J. G.; da Silva, C. V.; Cerqueira, D. A. Thermal Analysis and FTIR Studies of Sewage Sludge Produced in Treatment Plants. The Case of Sludge in the City of UberlâNdia-MG, Brazil. *Thermochim. Acta* **2012**, *528*, 72−75.
(30) Yanfen, L.; Xiaoqian, M. Thermogravimetric Analysis of the Co-Combustion of Coal and Paper Mill Sludge. *Appl. Energy* **2010**, *87* (11), 3526−3532.
(31) Zhu, X.; Chen, Z.; Xiao, B.; Hu, Z.; Hu, M.; Liu, C.; Zhang, Q. Co-Pyrolysis Behaviors and Kinetics of Sewage Sludge and Pine Sawdust Blends under Non-Isothermal Conditions. *J. Therm. Anal. Calorim.* **2015**, *119* (3), 2269−2279.
(32) Bennadji, H.; Khachatryan, L.; Lomnicki, S. M. Kinetic Modeling of Cellulose Fractional Pyrolysis. *Energy Fuels* **2018**, *32* (3), 3436−3446.
(33) Liu, X.-L.; Cao, B.; Wang, S.; Ji, H.-F.; Hu, Y.-M.; Wang, Q. TG-MS-FTIR Analysis of Co-combustion of Enteromorpha and Rice Husk. *J. Jiangsu Univ., Nat. Sci. Ed.* **2017**, *38* (2), 155−160.
(34) Madarász, J.; Varga, P. P.; Pokol, G. Evolved Gas Analyses (TG/DTA−MS and TG−FTIR) on Dehydration and Pyrolysis of Magnesium Nitrate Hexahydrate in Air and Nitrogen. *J. Anal. Appl. Pyrolysis* **2007**, *79* (1), 475−478.
(35) Sadhukhan, A. K.; Gupta, P.; Goyal, T.; Saha, R. K. Modelling of Pyrolysis of Coal−biomass Blends Using Thermogravimetric Analysis. *Bioresour. Technol.* **2008**, *99* (17), 8022−8026.
(36) Aboyade, A. O.; Hugo, T. J.; Carrier, M.; Meyer, E. L.; Stahl, R.; Knoetze, J. H.; Görgens, J. F. Non-Isothermal Kinetic Analysis of the Devolatilization of Corn Cobs and Sugar Cane Bagasse in an Inert Atmosphere. *Thermochim. Acta* **2011**, *517* (1−2), 81−89.
(37) Balasundram, V.; Ibrahim, N.; Kasmani, R. M.; Hamid, M. K. A.; Isha, R.; Hasbullah, H.; Ali, R. R. Thermogravimetric Catalytic Pyrolysis and Kinetic Studies of Coconut Copra and Rice Husk for Possible Maximum Production of Pyrolysis Oil. *J. Cleaner Prod.* **2017**, *167*, 218−228.
(38) Kim, Y. S.; Kim, Y. S.; Kim, S. H. Investigation of Thermodynamic Parameters in the Thermal Decomposition of Plastic Waste−Waste Lube Oil Compounds. *Environ. Sci. Technol.* **2010**, *44* (13), 5313−5317.
(39) Ruvolo-Filho, A.; Curti, P. S. Chemical Kinetic Model and Thermodynamic Compensation Effect of Alkaline Hydrolysis of Waste Poly(Ethylene Terephthalate) in Nonaqueous Ethylene Glycol Solution. *Ind. Eng. Chem. Res.* **2006**, *45* (24), 7985−7996.
(40) Xu, Y.; Chen, B. Investigation of Thermodynamic Parameters in the Pyrolysis Conversion of Biomass and Manure to Biochars Using Thermogravimetric Analysis. *Bioresour. Technol.* **2013**, *146*, 485−493.

DOI: 10.1021/acs.energyfuels.8b01972
Energy Fuels 2018, 32, 9551−9558